JOURNAL OF SPACECRAFT AND ROCKETS
Vol. 35, No. 2, March–April 1998

Improved Methodology for Axial Force Prediction at Angle of Attack

F. G. Moore* and T. C. Hymer†
U.S. Naval Surface Warfare Center, Dahlgren, Virginia 22448-5000

An improved semiempirical method for axial force calculation on missile configurations has been developed. The method uses the theoretical methods currently used in the U.S. Naval Surface Warfare Center's aeroprediction code for zero angle-of-attack axial force computations and several wind-tunnel databases to compute changes in axial force at angle of attack. The method is applicable to bodies alone, wing–body, and wing–body–tail configurations for both zero and nonzero control deflections. It has been developed to allow computation for angle of attack up to 90 deg at Mach numbers up to 20. However, it has been validated against data only to Mach number of 4.6 and angle of attack to 40 deg for all configurations. For body alone and wing–body cases, it has been validated to 90 deg angle of attack. Additional test data or Navier–Stokes computations would allow refinement of the improved method. The new method has been compared with several existing techniques. The method was found to be as good as or better than existing techniques but more general than existing methods in terms of configurations and Mach numbers allowed for the method to be used.

Nomenclature

A, B, C, D	= variables used in definition of $f(M, \alpha)$ parameter, 1/rad
C_A	= total axial force coefficient
C_{A_B}	= that part of the axial force coefficient due to the base of the configuration
C_{A_f}	= that part of the axial force coefficient due to skin friction
C_{A_P}	= that part of the axial force coefficient due to pressure on the body excluding the base region
C_{A_α}	= total axial force coefficient component due to angle of attack (AOA)
C_{A_δ}	= axial force coefficient component due to control deflection, δ
C_{A_0}	= total axial force coefficient at AOA of zero degrees
C_D	= drag coefficient
C_L	= lift coefficient
$C_{N_{T(V)}}$	= normal force coefficient on tail due to wing shed vortices
$C_{N_{W(B)}}, C_{N_{T(B)}}$	= normal force coefficient of wing or tail, respectively, in presence of body
$f(M, \alpha)$, $f'(M, \alpha)$	= function and its derivative, respectively, which are defined based on various databases as a function of Mach number and AOA
$k_{W(B)}, k_{B(W)}$	= wing–body and body–wing interference factors, respectively, due to control deflection at 0-deg angle of attack
L/D	= lift-to-drag ratio
M, M_∞	= Mach number and freestream Mach numbers
α	= angle of attack, deg
δ	= control deflection with leading edge up as positive, deg
Φ	= roll position, deg, with $\Phi = 0$ deg having fins in plus (+) roll orientation and $\Phi = 45$ deg having fins in cross (×) roll position

Received March 28, 1997; revision received Aug. 18, 1997; accepted for publication Oct. 10, 1997.

*Senior Aerodynamicist, Weapons Systems Department, Dahlgren Division. Associate Fellow AIAA.

†Aerospace Engineer, Aeromechanics Branch, Weapons Systems Department, Dahlgren Division.

Introduction

THE latest version of the aeroprediction code (AP95) (Ref. 1) available to the public emphasizes zero lift drag or axial force coefficient at zero angle of attack (AOA) with only minor attention devoted to the change in C_A with AOA. One component of C_A is treated in a fairly comprehensive manner. The primary rationale for not devoting more effort to calculating the change in total axial force with AOA is the fact that, for most conditions, normal force is the dominant term in lift, drag, and lift/drag ratio at high AOA, and C_A plays a secondary role. However, at subsonic Mach numbers, C_A can actually go negative at high AOA, causing more error in C_L, C_D, and L/D than desired. Also, at very high Mach numbers ($M > 3.0$), C_A tends to increase with AOA much more than the current AP95 predicts. Finally, the change in C_A with control deflection, although predicted reasonably well by the AP95, could possibly be improved somewhat, also at subsonic and high supersonic conditions. It is therefore the intent of this paper to discuss the physics of the changes in axial force with AOA, to develop a semiempirical mathematical model to account for the physics, and to compare the improved axial force model at AOA with the AP95 and experimental data.

In researching the literature for methods to account for axial force changes with AOA, we found three. The first of these was by Jorgensen,[2] where he approximated C_A by

$$C_A \simeq C_{A_0} \cos^2 \alpha, \qquad 0 \le \alpha \le 90 \text{ deg} \tag{1}$$

This method worked reasonably well for subsonic Mach numbers and AOAs less than about 30 deg. References 3 and 4 improved upon the Jorgensen method by assuming

$$C_A = C_{A_0} + f(M, \alpha) \tag{2}$$

where $f(M, \alpha)$ (Ref. 3) was approximated by a fourth-order polynomial in AOA for subsonic and transonic Mach numbers and was assumed to be zero[4] for supersonic Mach numbers. The efforts of Refs. 3 and 4 were an improvement on the Jorgensen methodology at all Mach numbers and particularly for AOAs greater than about 30 deg. However, because $f(M, \alpha) = 0$ at $M \ge 1.5$, the method did not pick up the increase in C_A due to compressibility effects at higher M. Reference 5 then improved upon Ref. 4 by assuming $f(M, \alpha)$ was second order in AOA at supersonic Mach numbers for bodies alone and third order for wing–bodies. Unlike Ref. 1, which gives consistently accurate results for C_{A_0}, using second-order methods, Refs. 2–5 use basically empirical methods for computing C_{A_0}. The fact that C_{A_0} was estimated empirically means the empirical

methods are limited to the databases on which they are based, not only at high AOA but at low AOA as well. Furthermore, neither Ref. 4 nor Ref. 5 treated wing–body–tail configurations separately from wing–body cases.

Although Refs. 4 and 5 give acceptable accuracy for $f(M, \alpha)$ at AOAs to 90 deg for body alone and body–tail cases, they use different prediction methods in various Mach number regions. It is the goal of the present work to derive a single new function, $f(M, \alpha)$, that is as accurate or more accurate than either the Ref. 4 or Ref. 5 methods yet is applicable over the entire Mach number and AOA range of interest and is applicable to body alone, wing–body, or wing–body–tail cases. In addition, neither Refs. 2, 4, nor 5 treated empirical corrections to axial force on missile configurations with combined AOA and control deflection. This area will also be investigated for possible improvement. The technology discussed in this paper will be included as part of the next version of the aeroprediction code (AP98) to be released to the public in 1998.

Analysis

C_{A_0} Methodology

The methods used in the AP95 to calculate C_{A_0} have been well documented (see Refs. 1 and 6–12) and will not be discussed here. Suffice it to say that a major effort has been placed on obtaining accurate estimates of C_{A_0} from the inception of the aeroprediction code in 1972 to the present. A general class of configurations are allowed with nose shapes that can be pointed, blunt, or truncated with one other slope discontinuity along the nose allowed. The afterbody is cylindrical with either a boattail or flare allowed as well. Most of the methods used are analytical, and many are second order accurate for wave drag calculations. As a result of this level of detail given to the zero lift drag force computations, average accuracy levels on C_{A_0} of $\pm 10\%$ have been obtained from the first version of the aeroprediction code (AP72) to the latest version available to the public (AP95).

C_A Physical Phenomena at AOA

Before we develop a mathematical model to address changes in axial force coefficient as a function of AOA, it is appropriate to discuss the physics of the flow that causes these changes. To visualize the changes, the axial force will be once again broken down into its components due to pressure, skin friction, and base drag.

For subsonic Mach numbers and spherically blunt or ogive-shaped bodies, the pressure drag at low-to-moderate AOA is zero. However, as AOA is increased or for bodies with truncated noses or large cone half-angles, the flow forms a separation bubble in the vicinity of the nose region. This separation bubble has a negative pressure coefficient, which means the axial force decreases with AOA. On the other hand, at high Mach numbers, the pressure coefficient on the windward side of the body is a function of the sine squared of the angle between a tangent to the body surface and the velocity vector. This means the increase in axial force at high Mach numbers with AOA is positive due to compressibility effects of the air. On the leeward surface of the body, the pressure coefficient approaches zero at high Mach numbers so that it has little effect on the axial force coefficient. None of the theoretical methods being used for computing the pressure component of the axial force coefficient accurately account for these changes above AOA of about 10 deg.

The base axial force changes with AOA are positive at all Mach numbers[12] but are the largest at transonic Mach numbers. At very high Mach numbers where the base term approaches zero, the change with AOA is also zero. At moderate AOA, the increase in base axial force reaches a maximum and then begins decreasing with additional increases in AOA. When fins are placed on the body in the vicinity of the base, the increase in base axial force with AOA is mitigated substantially. The phenomena that cause these effects with AOA are not clear. It is suspected that for the body alone, the initial AOA increases cause a stronger separation at the shoulder due to a larger turn angle at the base. However, when fins are placed in the vicinity of the base, it is suspected that some of the high dynamic pressure fluid is channeled into the base region, thus mitigating the negative base pressure coefficient somewhat.

The skin-friction coefficient axial force change with AOA is even harder to estimate or to explain due to the lack of computational fluid dynamics or wind-tunnel data that attempt to measure this quantity at moderate to high AOA. At lower Mach numbers, where strong separation exists in the leeward plane area along with a fairly large reverse flow region, it is suspected that the skin friction decreases with AOA. As the Mach number increases, the reverse flow region decreases and the change in skin-friction axial force with AOA is probably nearly constant or maybe slightly positive for low-to-moderate AOAs.

Another physical phenomenon that causes changes in C_A (at moderate and higher supersonic Mach numbers) with AOA is internal shock interactions. These phenomena are primarily associated with bodies with lifting surfaces and particularly those with more than one set. The body alone generally will have only a bow shock and internal expansion waves unless there is a surface discontinuity present. A body–tail configuration will have shocks coming off the tail surfaces, which interact with the bow shock. At Mach numbers and AOAs high enough, these interactions can have an impact on the axial force. Finally, if two or more sets of lifting surfaces are present, even stronger shock interactions occur between not only the bow and wing shock but also the wing to tail shocks as well. The situation is further complicated if a control surface is deflected. The internal shock interaction effects can affect the other static aerodynamics as well as axial force when this is the case.

Improved Semiempirical AOA Theoretical Model

As stated in the Introduction, the goal is to develop a single method that predicts $f(M, \alpha)$ of Eq. (2) as accurately as either of the methods in Refs. 4 and 5 but that applies for all Mach numbers for bodies with and without lifting surfaces and for AOA to 90 deg. To this end, we assume

$$f(M, \alpha) = A\alpha + B\alpha^2 + C\alpha^3 + D\alpha^4 \tag{3}$$

To evaluate the coefficients A, B, C, and D requires four independent conditions. Condition 1 is

$$\left.\frac{\partial f}{\partial \alpha}\right|_{\alpha=0} = f'(M, 0)$$

and for conditions 2–4 the value of $f(M, \alpha)$ is at $\alpha = 30$, 60, and 90 deg, respectively.

Using these four conditions, and putting α in radians vs degrees, we arrive at four equations to solve simultaneously.

Simultaneous solution of the variables A, B, C, and D from these four equations gives

$$\begin{aligned}
A &= f'(M, 0)\\
B &= -3.509 f'(M, 0) + 11.005 f(M, 30)\\
&\quad - 2.757 f(M, 60) + 0.41 f(M, 90)\\
C &= 3.675 f'(M, 0) - 17.591 f(M, 30)\\
&\quad + 7.041 f(M, 60) - 1.179 f(M, 90)\\
D &= -1.181 f'(M, 0) + 6.771 f(M, 30)\\
&\quad - 3.381 f(M, 60) + 0.752 f(M, 90)
\end{aligned} \tag{4}$$

Knowing $f'(M, 0)$, $f(M, 30)$, $f(M, 60)$, and $f(M, 90)$ in conjunction with Eqs. (2–4), improved estimates of C_A at AOAs up to 90 deg should be obtained. In reality, if the body is symmetric, then this AOA should be ± 90 as long as Eq. (3) is viewed in terms of absolute values for AOA.

The question that must be addressed is how to determine values of the parameters $f'(M, 0)$, $f(M, 30)$, $f(M, 60)$, and $f(M, 90)$. To do this, two large wind-tunnel databases were utilized. These were the NASA Tri-Service Data Base,[13] which contains detailed missile component data to AOA 45 deg, and the Baker[14] high AOA data base, which includes missile component data to 180 deg AOA. Reference 13 was used primarily for the lower AOA information, $f'(M, 0)$ and $f(M, 30)$, and Ref. 14 was used for the higher AOA variables, $f(M, 60)$ and $f(M, 90)$. The reason for this was that

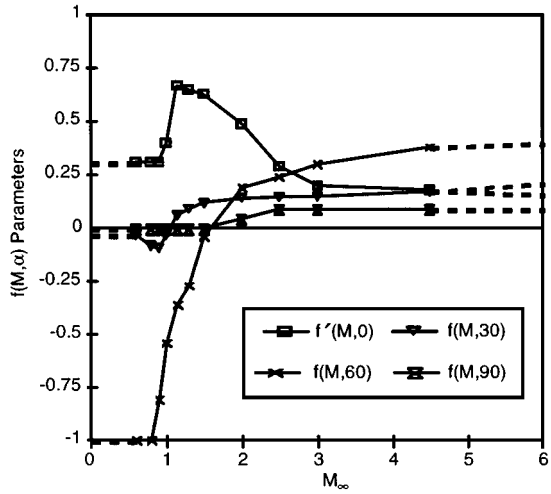

Fig. 1 Axial force AOA variation parameters for body alone.

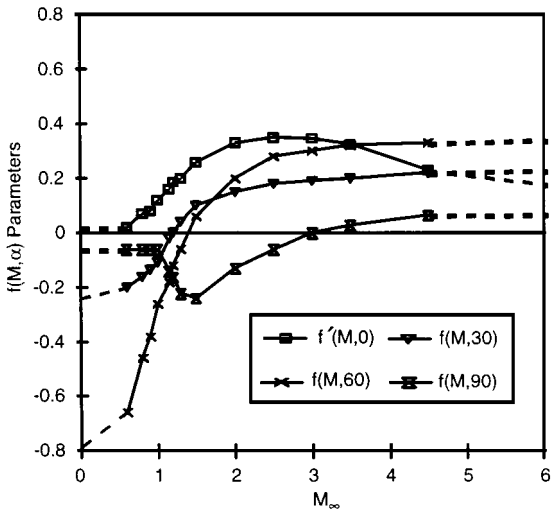

Fig. 2 Axial force AOA variation parameters for a body–tail configuration.

Ref. 13 data were available in tabular form, making the estimates of the parameters more accurate than from the Ref. 14 information, which was available only in graphs. For some data points in the transonic flow region, the parameter $f(M, 30)$ was obtained by averaging the data from both Refs. 13 and 14.

Figure 1 gives the values of the parameters $f'(M, 0)$, $f(M, 30)$, $f(M, 60)$, and $f(M, 90)$ for the body alone. Reference 5 indicated that analysis showed that the first parameter $[f'(M, 0)]$ was independent of nose length, nose shape, and total body length and dependent only on the Mach number. This assumption will also be made for the other three parameters as well. Comparison of the new method on configurations different from those within the database will determine the validity of this assumption.

Figure 2 gives the values of the same parameters for a configuration with one set of lifting surfaces. These parameters were derived mostly for body–tail configurations. In comparing values of the parameters in Fig. 2 with those of Fig. 1, it is seen that similar values exist for each parameter but they are slightly different. The Ref. 4 method shows no difference between configurations that are bodies alone vs those with lifting surfaces, and Ref. 5 shows a difference only as AOA approaches 90 deg. Thus the present method will also give slightly different results for body alone and wing–body or body–tail missile configurations than those of Refs. 4 and 5 due to differences in the values of the parameters used in defining the nonlinearity with AOA. This is in addition to differences arising from the use of a single equation for all cases in the present approach vs three different equations used in Refs. 4 and 5.

Unfortunately, neither of the databases given in Refs. 13 or 14 tested configurations with two sets of lifting surfaces. Although the

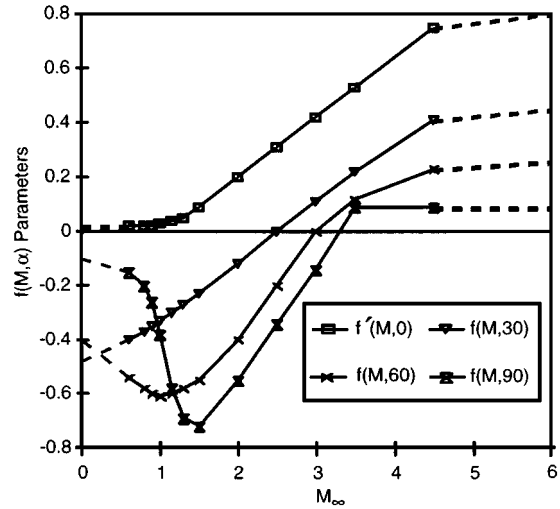

Fig. 3 Axial force AOA variation parameters for a wing–body–tail configuration.

coefficients defined by Fig. 2 could be used as an approximation for configurations with two sets of lifting surfaces, it will be attempted to improve upon these, at least for the lower AOAs where other data are available. To this end, Refs. 15–18 were utilized. References 15 and 16 were very helpful in defining $f'(M, 0)$ and $f(M, 30)$ for Mach numbers 0.8–4.6. Above 4.6, values of these parameters were extrapolated as was done in Figs. 1 and 2 as well. References 17 and 18 were utilized for low Mach number values of $f'(M, 0)$, $f(M, 30)$, and $f(M, 60)$. For high Mach numbers $f(M, 60)$ could be extrapolated reasonably well based on the Ref. 16 data in conjunction with Fig. 2. The $f(M, 90)$ data are simply a best guess based on $f(M, 60)$ values for wing–body–tail cases and $f(M, 60)$ and $f(M, 90)$ values of Fig. 2.

Values of the four parameters of Eq. (4) are given in Fig. 3 for configurations having two sets of lifting surfaces. In comparing Figs. 2 and 3, it is seen there are some similarities but also some differences. At low Mach numbers, trends of all four parameters are similar, which means that Fig. 2 could be used successfully for configurations with more than one set of lifting surfaces and still get reasonably accurate estimates of axial force change with AOA. This is in fact what Refs. 4 and 5 both do. However, as the Mach number increases, the values of the parameters $f'(M, 0)$ and $f(M, 30)$ tend to be higher for two sets of lifting surfaces compared with one. That is, C_A increases faster and reaches a higher peak value with AOA for a wing–body–tail case than for a wing–body or body–tail case.

The last physical phenomenon to be modeled is the change in axial force coefficient with control deflection as AOA increases. The AP95 defines the axial force term due to control deflection as

$$C_{A_{\delta_W}} = C_{N_{W(B)}} \sin \delta_W \tag{5a}$$

for the forward lifting surface and as

$$C_{A_{\delta_T}} = \left[C_{N_{T(B)}} + C_{N_{T(V)}}\right] \sin \delta_T \tag{5b}$$

for a rearward lifting surface if two sets of lifting surfaces are present. If only one set of lifting surfaces is present, Eq. (5a) applies regardless of the fin location. Equation (5b) contains the tail interference term as a result of the forward set of fins, whereas Eq. (5a) does not have this term. Both $C_{N_{W(B)}}$ and $C_{N_{T(B)}}$ of Eq. (5) are the normal force coefficient on the wing or tail due to both AOA and control deflection.

In analyzing Eqs. (5a) and (5b), they both basically assume that the axial force due to control deflection is simply the normal force of the wing in conjunction with the body times the sine of the control deflection angle δ. In examining comparisons of this approach to data, it was found that, when α and δ were of the same sign, Eq. (5) gave agreement with experimental data, which was quite acceptable. However, when α and δ were of opposite signs, it was found the agreement was not as good as desired for higher Mach numbers. It

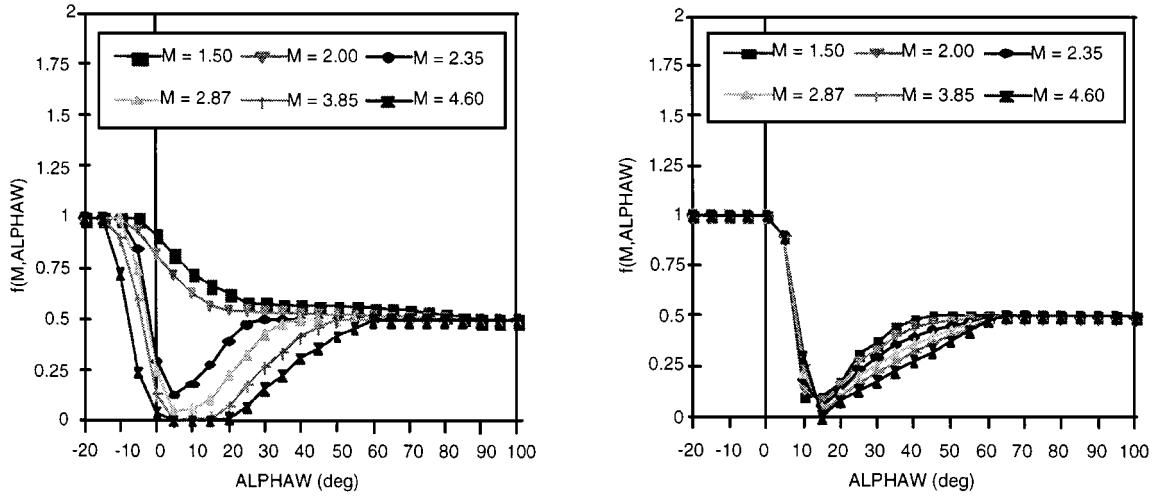

a) Φ = 0 deg b) Φ = 45 deg

Fig. 4 Values of $f(M, \alpha_W)$ for α and δ of opposite signs.

is suspected that part of the reason for this is the nonlinear model of $k_{W(B)}$ and $k_{B(W)}$ is accurate for α and δ of the same sign, but when α and δ are of opposite signs, the total values of $k_{W(B)}$ and $k_{B(W)}$ are correct, but each may be in error, and the errors tend to compensate. It is speculated that the fundamental source of this discrepancy is wing gap effects when the wings are deflected. This cancellation of errors could give accurate normal force but possibly inaccurate axial force contributions due to AOA.

Because no direct data measurements are available and because the control deflection matrix of Ref. 1 gives quite acceptable values of normal force and pitching moment, the approach taken here is to define a term $f(M, \alpha_W)$ by which to multiply Eq. (5) when α and δ are of opposite signs.

Then

$$C_{A_{\delta_W}} = \left[C_{N_{W(B)}} \sin \delta_W\right] f(M, \alpha_W) \tag{6a}$$

and

$$C_{A_{\delta_T}} = \left[C_{N_{T(B)}} + C_{N_{T(V)}}\right] \sin \delta_T \, f(M, \alpha_T) \tag{6b}$$

where α_W and α_T of Eq. (6) are defined by

$$\alpha_W = \alpha + \delta_W, \qquad \alpha_T = \alpha + \delta_T \tag{7}$$

Because the generic wind-tunnel databases available have fins that are too small to accurately determine $f(M, \alpha)$, use of other databases[16,18] in conjunction with the AP95 code will be used instead. Figure 4a gives values of $f(M, \alpha_W)$ for Mach numbers between 1.5 and 4.60 at $\Phi = 0$, and Fig. 4b gives the complementary values at $\Phi = 45$ deg. For Mach numbers above 4.6, the values at 4.6 are used. For Mach numbers below 1.5, $f(M, \alpha_W)$ is assumed to go to its value of 1.0 at $M_\infty = 0.8$ and remain at that value below that Mach number. This assumption again is based on comparisons to data at low speeds. For α and δ of the same sign, $f(M, \alpha_W)$ is always 1.0.

The value of $f(M, \alpha_W)$ at $\alpha_W = 90$ deg has been assumed to be 0.5 for both the $\Phi = 0$- and 45-deg planes. If the wing were not in the presence of the body, then a value of 1.0 would be natural at least at $\Phi = 0$. However, due to body interference, the full effect of control deflection on $f(M, \alpha_W)$ at α_W does not appear to be obtained at $\alpha_W = 90$ deg based on extrapolated experimental data at lower values of α_W. Hence, the assumed value of 0.5. Hopefully, higher AOA experimental data that can be used to improve upon this assumption will become available.

Results and Discussion

Several body alone, wing–body and wing–body–tail configurations are considered in Ref. 19, which is the detailed technical report upon which this paper is based. Only a selected sampling of results will be shown here. These results will illustrate the comparison of the new method to that of Refs. 2–5 for a body alone and body–tail case and will illustrate results for a wing–body–tail case with control deflection, for which Refs. 2–5 were not directly applicable.

The first case considered is one of the body-alone configurations tested by Baker.[14] The Baker database was the primary database on which the theoretical axial force methods of Refs. 3–5 were based. This database consisted of several body-alone and body–tail configurations tested at AOAs to 180 deg and Mach numbers 0.6–3.0. Figure 5a shows the body alone and body–tail considered as an example here. The body has a 2.5-caliber tangent ogive nose and 7.5-caliber cylindrical afterbody. The tail planform has an aspect ratio of one. The configuration was tested with a boundary-layer trip at a Reynolds number of 4×10^6/ft. Hence, the option in the aeroprediction code for a wind-tunnel model with boundary-layer trip is used to compute C_{A_0} for the given test Reynold's number. Of course, C_{A_α} is not assumed to be affected by either the Reynolds number or the state of the boundary layer.

Figure 5b compares the new theoretical approach with the body-alone axial force data of Ref. 14. Also shown on Fig. 5b for the lower Mach number cases is the fourth-order axial force method of Ref. 4 and the third-order method of Ref. 5 for the higher Mach number cases. Note that the new method achieves one of its objectives of being as accurate as the Refs. 4 and 5 methods while using a single method vs dual methods. One of the reasons the Refs. 4 and 5 methods compare as well as they do to data is that the C_{A_0} prediction of those references is based on the Baker database. The new method uses AP95 theoretical methodology to predict C_{A_0} and still gives as good or better comparison to the Baker[14] data than either Ref. 3 or Ref. 4.

Figure 5c compares the predictions of the new theory to the Baker data and the method of Ingram et al.[5] at several supersonic Mach numbers for the body–tail configuration of Fig. 5a. Note that both the third order[5] and the present fourth order in AOA methods predict C_{A_α} quite well for supersonic Mach numbers. However, although not shown in Fig. 5c, the third-order AOA method does not work well at subsonic Mach numbers.

In examining the comparisons of the new method of this report to those of Refs. 3–5 in Fig. 5, it is seen that one of the objectives of this work has been achieved. That is, a single method (vs multiple methods) has been defined that works as well as or better than those available[3–5] for body-alone and body–tail configurations over the entire Mach number range and for AOAs to 90 deg. The method has been validated for a more limited Mach number range due to availability of data, however.

References 3–5 derived nonlinear AOA predictors for C_A for body-alone and body–tail configurations. No consideration was given to configurations with more than one set of lifting surfaces or to control deflections and so the user of this technology is left with the use of body–tail methodology for configurations with more than one set of lifting surfaces. The next example will apply the present

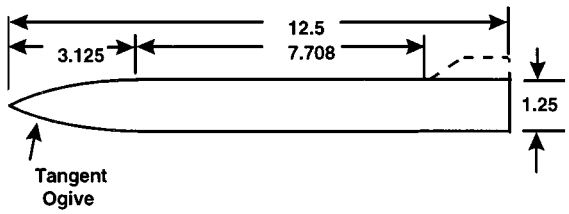

Fig. 5a Body-alone and one body-tail configuration of Baker database[14] (dimensions in inches).

new method of predicting C_{A_α} for configurations with more than one set of lifting surfaces. The theory for these examples is based on AP95 methods at AOA = 0, Eqs. (2) and (3), along with Fig. 3 for no control deflection or when α and δ are of the same sign.

The configuration chosen to illustrate the wing–body–tail methodology is shown in Fig. 6a, with the experimental results given in Ref. 17. This configuration has a length of about 18 calibers with a tangent ogive nose of 2.25 calibers in length. It has wings and tails of fairly high aspect ratios of 2.8 and 2.6, respectively. Data were taken at Mach numbers 1.5–4.63, for AOAs to 45 deg, and control

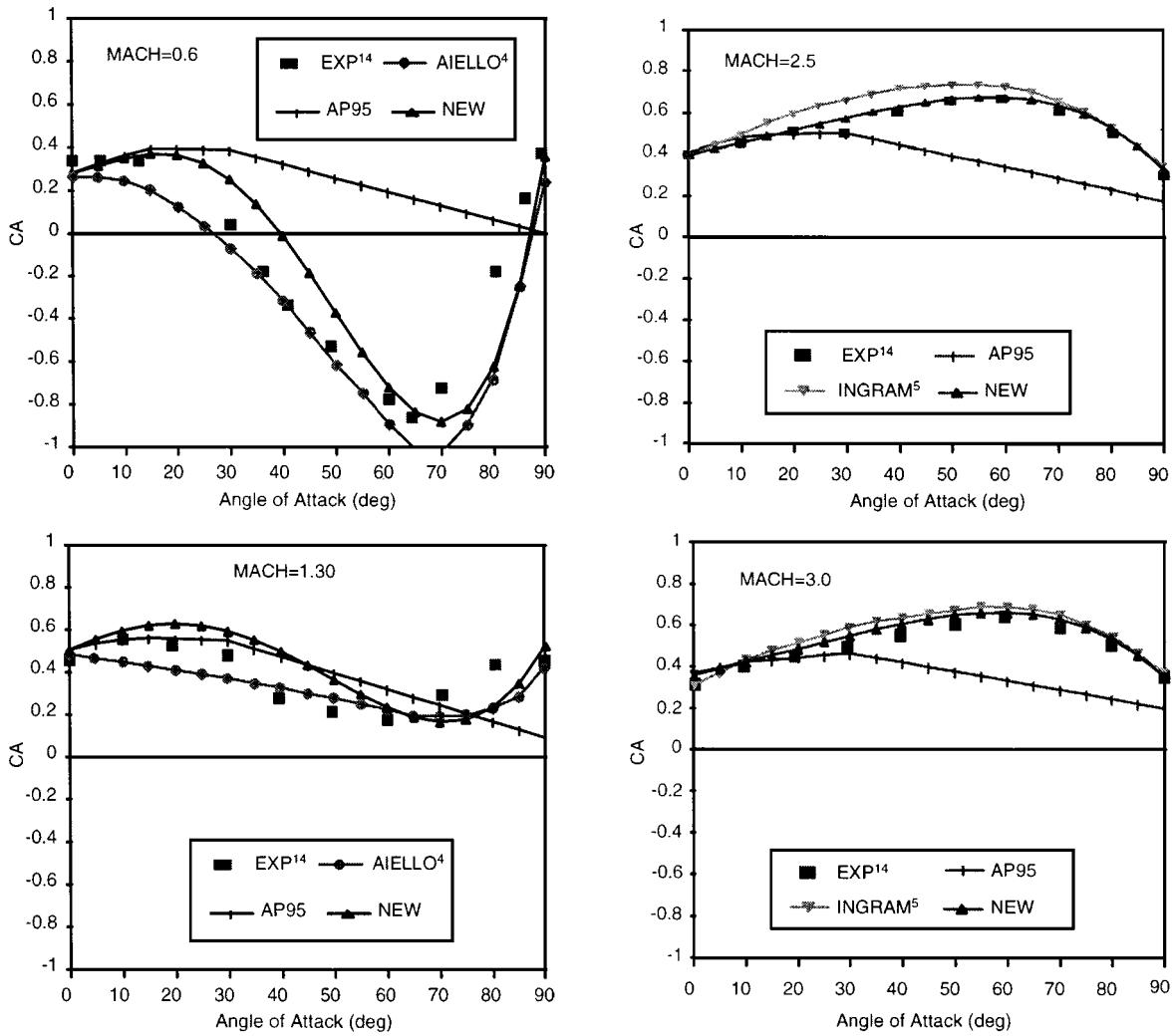

Fig. 5b Comparison of axial force coefficients of theory and experiment[14] for body alone of Fig. 5a.

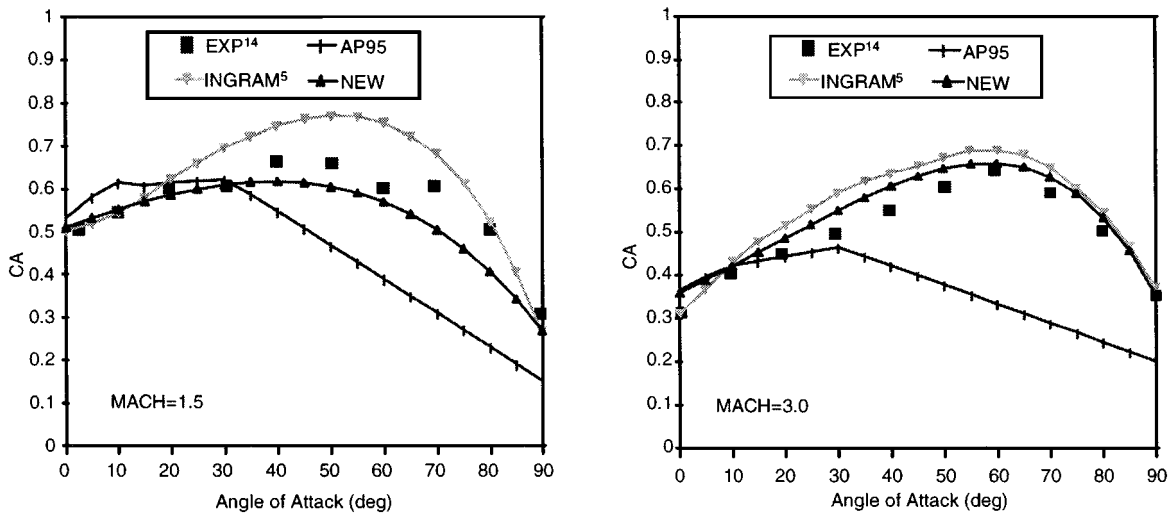

Fig. 5c Comparison of axial force coefficients of theory and experiment[14] for body–tail configuration of Fig. 5a.

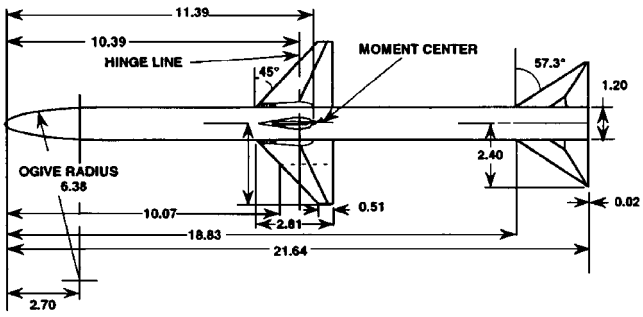

Fig. 6a Wing-body-tail missile configuration used in validation.[17]

deflections of 0 and 10 deg at Mach numbers of 1.5 and 2.0 and 0–20 deg at Mach numbers of 2.35 to 4.63. The data were taken at a Reynolds number of 2.5×10^6/ft and boundary-layer trips were also used. The model had a hollow chamber, and chamber axial force measurements were given separately in Ref. 17. These results were added to the forebody axial force measurements to compare with the AP95 and the new AOA axial force prediction method presented in this report.

Figures 6b–6d show the comparisons of the new theory with the previous AP95 calculations and the data of Ref. 17. Mach numbers 1.5 and 4.6 are shown in the comparisons.

Figure 6b is the 0-deg control deflection results at $\Phi = 0$. Figures 6c and 6d give the corresponding comparisons of theory to data[17] for

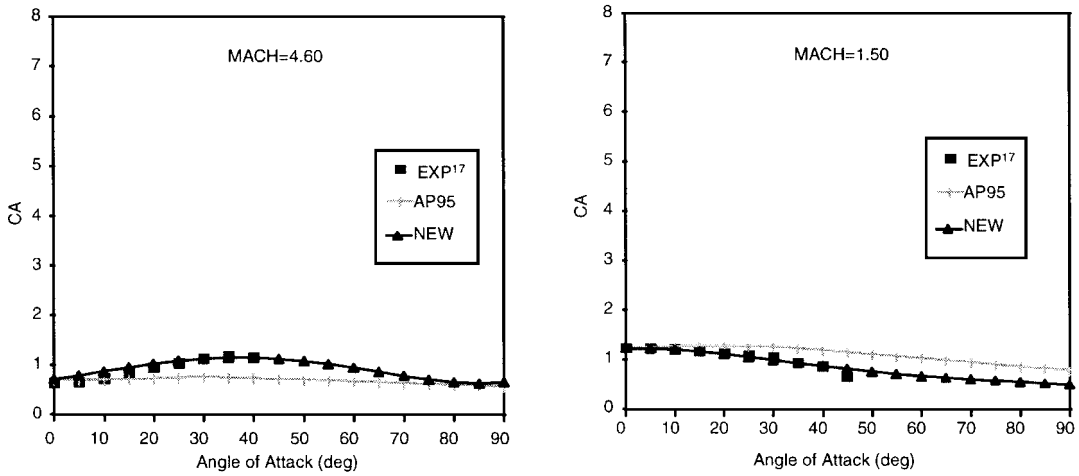

Fig. 6b Comparison of theory and experiment[17] for configuration of Fig. 6a ($\Phi = 0$ deg and $\delta = 0$ deg).

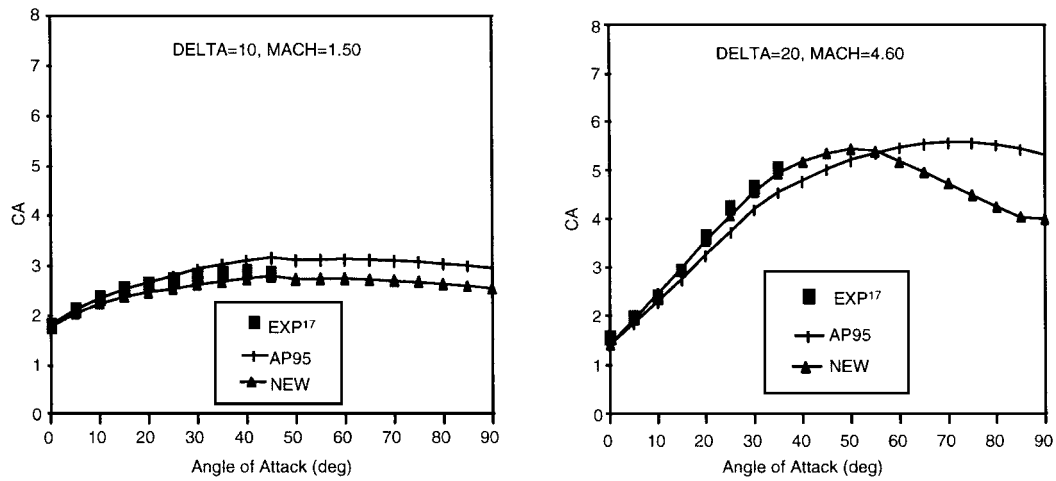

Fig. 6c Comparison of theory and experiment[17] for configuration of Fig. 6a ($\Phi = 0$ deg).

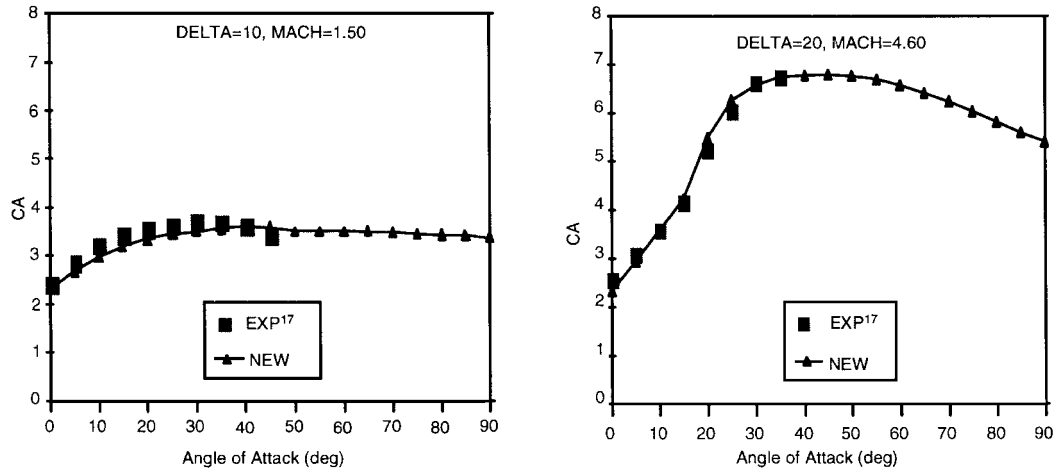

Fig. 6d Comparison of theory and experiment[17] for configuration of Fig. 6a ($\Phi = 45$ deg).

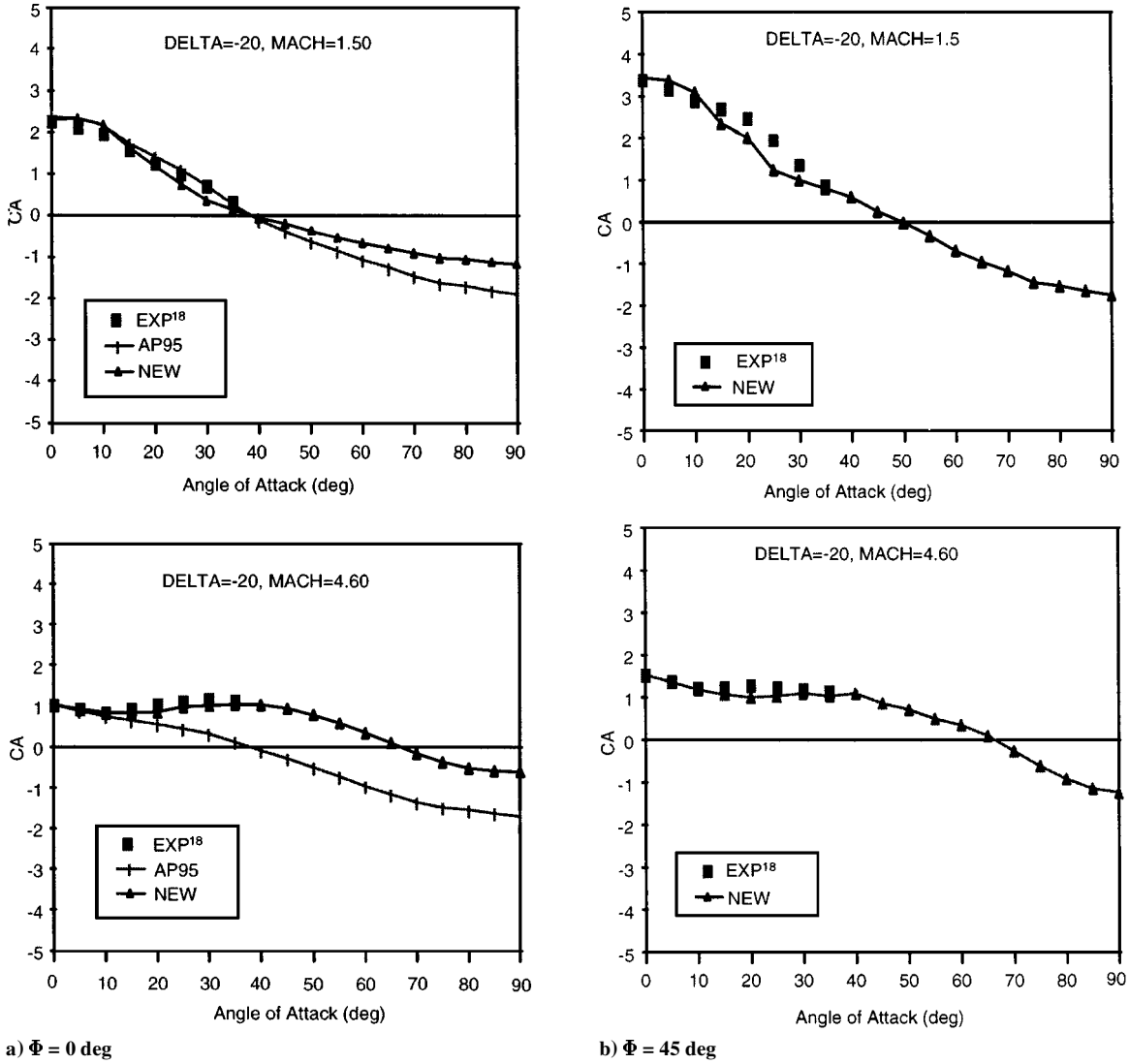

a) Φ = 0 deg b) Φ = 45 deg

Fig. 7 Comparison of axial force coefficients of a tail-controlled wing–body–tail configuration.[18]

$\Phi = 0$- and 45-deg roll, respectively, but with control deflection. At $M_\infty = 1.5$, the control deflection is 10 deg, whereas at $M_\infty = 4.6$, it is 20 deg. Here the theory distinguishes between roll of 0 and 45 deg, because only two fins are deflected at 0-deg roll, whereas all four are deflected at 45-deg roll. Also note that no AP95 computations are shown on Fig. 6d because the AP95 is only applicable at $\Phi = 0$ deg. Note that in Figs. 6b–6d, the new method in general is equal to or superior to the AP95 and also gives very good agreement in comparison to data. The average accuracy errors of the new method to data in Figs. 6b–6d are well within the $\pm 10\%$ accuracy level claimed in the overall accuracy levels for normal and axial force coefficients.

The final configuration considered for validation is a wing–body–tail case where the tail surfaces are used for control. The configuration is identical to the configuration in Fig. 6a except that the wing trailing edges are truncated with a height of 0.05 in. vs being sharp, as shown in Fig. 6a. This means the drag of this configuration is slightly greater than the wing-controlled case due to the wing trailing-edge base pressure drag. The wind-tunnel data[18] were taken at a Reynolds number of 2.0×10^6/ft vs the wing controlled case of 2.5×10^6/ft. However, a boundary-layer trip was used for both the tail and wing controlled models.

The comparisons of axial force coefficients to data[18] of the new method to the AP95 and experiment for no control deflection are quite similar to the results of Fig. 6b and therefore will not be repeated here. The results for $\delta = -20$ deg at $\Phi = 0$ and 45 deg are shown in Figs. 7a and 7b, respectively. Results are given in each figure for Mach numbers of 1.5 and 4.6. The theory is shown up to AOA 90 deg, although data are available only up to AOA of 35 deg. For Mach number of 1.5, both the AP95 and the new method appear to give acceptable results compared with data at $\Phi = 0$. However, for the higher Mach number, the new method is superior to the AP95. The reason for this improved performance is due to the empirical model for AOA and control deflection of opposite signs as given in Fig. 4. For the $\Phi = 45$-deg roll position, only the new method results are shown in Fig. 7b because the AP95 is not applicable to this roll position.

Summary

An improved semiempirical method for axial force calculation on missile configurations has been developed. The method uses the theoretical methods currently used in the 1995 version of the U.S. Naval Surface Warfare Center aeroprediction code (AP95) for zero AOA axial force calculations and wind-tunnel databases to compute changes in axial force at AOA for body-alone and wing–body configurations. Comparisons to data and existing theoretical approaches for computing the AOA contribution to axial force indicate the new method to be as good as or superior to existing techniques at all Mach numbers and AOAs. The improved method was also extended to configurations that have two sets of lifting surfaces and also to consider axial force due to control deflection. Comparisons of the extended method to the AP95 for wing–body–tail configurations showed improvements to the AP95 at higher AOA, at higher Mach numbers, and when the AOA and control deflection were of opposite sign.

In developing the improved semiempirical method, several assumptions were necessary: 1) the value of C_A at AOA of 90 deg for configurations with two sets of lifting surfaces and for configurations with control deflections, 2) the value of C_A at high AOA outside the Mach number range for which data were available ($M > 4.6$), and

3) how to break the contribution in C_A due to AOA into individual axial force components due to skin friction, wave, or pressure and base pressure.

Acknowledgments

The work described in this paper was supported through the U.S. Office of Naval Research (Dave Siegel) by the following programs: the Air Launched Weapons Program managed at the U.S. Naval Air Warfare Center, China Lake, California, by Tom Loftus and Craig Porter; the Surface Weapons Systems Technology Program managed at the U.S. Naval Surface Warfare Center, Dahlgren Division (NSWCDD), by Robin Staton and Gil Graff; and the Marine Corps Weaponry Technology Program managed at NSWCDD by Bob Stiegler. The authors express appreciation for support received in this work. Appreciation is also given to Roy McInville, who provided some assistance in the validation process.

References

[1]Moore, F. G., McInville, R. M., and Hymer, T., "The 1995 Version of the NSWC Aeroprediction Code: Part I—Summary of New Theoretical Methodology," U.S. Naval Surface Warfare Center, Dahlgren Div., NSWCDD/TR-94/379, Dahlgren, VA, Feb. 1995.

[2]Jorgensen, L. H., "Prediction of Static Aerodynamic Characteristics for Slender Bodies Alone and with Lifting Surfaces to Very High Angles of Attack," NASA TR R-474, Sept. 1977.

[3]Fidler, J. E., and Bateman, M. C., "Aerodynamic Methodology (Bodies With and Without Tails in Transonic Flow)," Naval Air Systems Command, Rept. issued under U.S. Navy NAVAIR Contract N00019-73-C-0108, Washington, DC, 1974.

[4]Aiello, G. F., and Bateman, M. C., "Aerodynamic Stability Technology for Maneuverable Missiles," Air Force Flight Dynamics Lab., U.S. Air Force Systems Command, AFFDL-TR-76-55, Vol. 1, Wright–Patterson AFB, OH, Dec. 1976.

[5]Ingram, C. W., Ball, K., Dinkeloo, C., and Shida, D., "Preliminary Design Aerodynamic Prediction Methodology for Missiles with Nose Bluntness," Air Force Flight Dynamics Lab., U.S. Air Force Systems Command, AFFDL-TR-78-117, Wright–Patterson AFB, OH, Sept. 1978.

[6]Moore, F. G., "Body Alone Aerodynamics of Guided and Unguided Projectiles at Subsonic, Transonic and Supersonic Mach Numbers," U.S. Naval Surface Warfare Center, Dahlgren Div., NWL TR 2796, Dahlgren, VA, Nov. 1972.

[7]DeJarnette, F. R., and Jones, K. M., "Development of a Computer Program to Calculate Aerodynamic Characteristics of Bodies and Wing–Body Combinations," U.S. Naval Surface Warfare Center, Dahlgren Div., NSWC/DL TR-3829, Dahlgren, VA, April 1978.

[8]Moore, F. G., Armistead, M. A., Rowles, S. H., and DeJarnette, F. R., "Second-Order, Shock Expansion Theory Extended to Include Real Gas Effects," U.S. Naval Surface Warfare Center, Dahlgren Div., NAVSWC TR-90-683, Dahlgren, VA, Feb. 1992.

[9]Wu, J. M., and Aoyoma, K., "Transonic Flow-Field Calculation Around Ogive Cylinders by Nonlinear-Linear Stretching Method," U.S. Army Missile Command, TR-70-12, Huntsville, AL, April 1970.

[10]Chaussee, D. S., "Improved Transonic Nose Drag Estimates for the NSWC Missile Aerodynamic Computer Program," U.S. Naval Surface Warfare Center, Dahlgren Div., NSWC/DL TR-3830, Dahlgren, VA, April 1978.

[11]Devan, L., "Aerodynamics of Tactical Weapons to Mach Number 8 and Angle of Attack 180°: Part I, Theory and Application," U.S. Naval Surface Warfare Center, Dahlgren Div., NSWC TR 80-346, Dahlgren, VA, Oct. 1980.

[12]Moore, F. G., Wilcox. F., and Hymer, T., "Improved Empirical Model for Base Drag Prediction on Missile Configurations Based on New Wind Tunnel Data," U.S. Naval Surface Warfare Center, Dahlgren Div., NSWCDD/TR-92/509, Dahlgren, VA, Oct. 1992.

[13]NASA Langley Research Center Tri-Service Missile Data Base, transmitted from Jerry M. Allen at NASA Langley Research Center, U.S. Naval Surface Warfare Center, Dahlgren Div., Nov. 1991 (formal documentation in process).

[14]Baker, W. B., "Static Aerodynamic Characteristics of a Series of Generalized Slender Bodies With and Without Fins at Mach Numbers from 0.6 to 3.0 and Angles of Attack from 0 to 180 Deg," Arnold Engineering and Devlopment Center, U.S. Air Force Systems Command, AEDC TR-75-125, Vols. 1 and 2, Arnold Air Force Station, TN, May 1976.

[15]Graves, E., and Fournier, R., "Stability and Control Characteristics at Mach Numbers of 0.2 to 4.63 of a Cruciform Air-to-Air Missile with Triangular Canard Controls and a Trapezoidal Wing," NASA TM-X 3070, Nov. 1974.

[16]Smith, E. H., Hebbar, S. K., and Platzer, M., "Aerodynamic Characteristics of a Canard-Controlled Missile at High Angles of Attack," AIAA Paper 93-0763, Jan. 1993.

[17]Monta, W. J., "Supersonic Aerodynamic Characteristics of a Sparrow III Type Missile Model with Wing Controls and Comparison with Existing Tail-Control Results," NASA TP 1078, Nov. 1977.

[18]Monta, W. J., "Supersonic Aerodynamic Characteristics of an Air-to-Air Missile Configuration with Cruciform Wings and In-Line Tail Controls," NASA TM S-2666, 1972.

[19]Moore, F. G., and Hymer, T., "An Improved Method for Predicting Axial Force at High Angle of Attack," U.S. Naval Surface Warfare Center, Dahlgren Div., NSWCDD/TR-96/240, Dahlgren, VA, Feb. 1997.

R. M. Cummings
Associate Editor